ГИАБ. Горный информационно-аналитический бюллетень /
MIAB. Mining Informational and Analytical Bulletin, 2021;(4-1):73—80
ОРИГИНАЛЬНАЯ СТАТЬЯ / ORIGINAL PAPER

УДК 539.431.1 + 621.7.01 DOI: 10.25018/0236_1493_2021_41_0_73

# ОБРАЗОВАНИЕ ДЕФЕКТОВ В СИНТЕТИЧЕСКИХ КРИСТАЛЛАХ КВАРЦА ПРИ ОДНОСОСНОМ СЖАТИИ

**Ян Прушка[1], А. Кравцов[1], И. Е. Сас[2], Е. Б. Черепецкая[2], Виего Жозе Викторина[2], Н. Г. Борисов[2]**

[1] Чешский технический университет в Праге, Чешская Республика;
[2] Национальный Исследовательский Технологический Университет «МИСиС» Горный институт, Москва, Россия

***Аннотация:*** В данной статье рассматривается возможность использования комплекса интроскопических методов, включающего акустическую эмиссию и лазерный ультразвуковой неразрушающий контроль для исследования поведения синтетических кристаллов кварца при циклической нагрузке. Эксперимент включал в себя два последовательных цикла нагружения, в ходе которых с помощью автоматизированного лазерно-ультразвукового структуроскопа ГЕОСКАН-2МУ исследовались прочностные свойства синтетического кварца и процесс образования дефектов внутренней структуры. Дальнейшая интерпретация экспериментальных результатов проводилась с помощью численного моделирования на основе модели Друкера-Прагера, которая описывает поведение среды при одноосном сжатии с учетом ее прочностных характеристик. В результате было установлено, что несмотря на небольшое количество дефектов и неоднородностей в образце в начале нагружения, активация процесса роста микротрещин начинается при внешней нагрузке 30 МПа. Это составляет около десяти процентов от разрушающего напряжения. Когда внешняя нагрузка достигает 75 МПа, в центральной части образца возникают микротрещины длиной более 20 мм. Результаты данного исследования могут быть использованы для создания численной модели, которая будет учитывать нелинейную зависимость деформаций и напряжений от внешней нагрузки.

***Ключевые слова:*** синтетический кварц, лазерный ультразвуковой контроль, акустическая эмиссия, структуроскоп, одноосное сжатие, микротрещина, численное моделирование, прочностные свойства.

***Для цитирования:*** *Ян Прушка, Кравцов А., Сас И. Е., Черепецкая Е. Б., Виего Жозе Викторина, Борисов Н. Г.* Образование дефектов в синтетических кристаллах кварца при одноосном сжатии // Горный информационно-аналитический бюллетень. — 2021. — № 4-1. — С. 73—80. DOI: 10.25018/0236_1493_2021_41_0_73.

## Defect formation in synthetic quartz crystals under uniaxial compression

**Jan Pruška[1] , A. N. Kravcov[1], I. E. Sas[2], E. B. Cherepetskaya[2], Viegas Jose Victorino[2], N. G. Borisov[2]**

[1] Czech Technical University in Prague, Faculty of Civil Engineering, Czech Republic
[2] National University of Science and Technology MISIS, Moscow, Russia

***Abstract:*** The paper discusses the possibility of using a complex of non-destructive acoustic emission and laser ultrasonic testing methods to study the behavior of synthetic quartz

crystals under cyclic loading. An automated laser ultrasonic structureroscope GEOSKAN-2MU was used to study the mechanical properties of synthetic quartz subjected to two successive loading cycles, monitoring the process of formation of defects in its internal structure. The experimental results were interpreted using numerical simulation based on the Drucker-Prager model, which describes the behavior of a medium under uniaxial compression, taking into account its strength characteristics. It is found that, despite the presence of a small number of defects and heterogeneities in the specimen before loading, the onset of microcrack growth occurs at an external load of 30 MPa, which is about ten percent of the failure stress. At an external load of 75 MPa, microcracks more than 20 mm long appear in the central part of the specimen. The results of this study can be used to develop a numerical model that will take into account the nonlinear dependence of deformations and stresses on the external load.

***Key words:*** synthetic quartz, laser ultrasonic testing, acoustic emission, structureroscope, uniaxial compression, microcrack, numerical simulation, strength properties.

***For citation:*** Jan Pruška, Kravcov A. N., Sas I. E., Cherepetskaya E. B., Viegas Jose Victorino, Borisov N. G. Defect formation in synthetic quartz crystals under uniaxial compression. *MIAB. Mining Inf. Anal. Bull.* 2021;(4-1):73–80. [In Russ]. DOI: 10.25018/0236_1493_2021_41_0_73.

## Introduction

The reliability and durability of buildings and other structures (including underground ones) is largely dependent on the geological conditions and the behavior of the rocks and soils under various additional mechanical loads [1–3]. Commonly encountered rocks are heterogeneous anisotropic media with defects of various sizes. Most studies of defect formation in different rocks under external mechanical loads [4–9] are carried out for practical applications; the nature of defect formation in geomaterials is scarcely investigated in a fundamental way.

In laboratory, the process of defect formation and its influence on the strength of natural rocks should be preferably studied on materials whose heterogeneous structure is similar to that of natural rocks, and which have controllable natural defects. One of such materials is synthetic quartz, an analog for natural quartz that is a mineral constituent of a large number of rocks [10, 11]. Synthetic quartz has a sufficiently uniform structure that can be controlled during the manufacturing. Synthetic quartz crystals, including those irradiated by protons and neutrons, are now widely used for various industrial applications. Systematic study of defect formation by nondestructive testing techniques will give generalized information about the mechanisms of defect initiation and propagation in natural rocks with a specific unique structure.

This paper discusses the use of the acoustic emission and laser-ultrasonic testing techniques to study the development of defects in synthetic quartz crystals under uniaxial mechanical load. The experimental results are compared with numerical simulation data.

## Experiment setups and basic computer modeling principles

Uniaxial compression experiments were carried out on structurally homogeneous samples of synthetic quartz (density $\rho$ = 2,65 g/sm$^3$) in the form of parallelepipeds with characteristic edge lengths: $a$ = 5 mm, $b$ = 2,5 mm and $c$ = 2,5 mm, the crystals having different elastic properties along the crystallophysical axes due to symmetry. Local heterogeneities in the samples (two-dimensional, one-dimensional, and point defects) were no more than $10^3$ см$^{-2}$ in size. The physical and mechanical properties of the test material before the testing are given in Table 1.

A manual press was used to perform cyclic compression testing of synthetic quartz at a constant speed of 2900 N/s. A special film was placed between the samples and the press plates to prevent friction. The maximum stress was 30 MPa (≈ $0{,}1\sigma_c$) in the first loading cycle and 79 MPa (≈ $0{,}27\sigma_c$) during the second one. The time interval between two loading cycles was 10 days. Acoustic emission during loading was registered by a piezoelectric ceramic sensor fixed on the sample. The acoustic signal generated by load-induced changes in synthetic quartz was converted into an electric signal to be fed to a computing unit. Registration was carried out in four frequency ranges: from 0 to 100 kHz, from 101 to 500 kHz, from 501 to 1000 kHz, and from 1001 to 5000 kHz. During the experiment, the number of times the acoustic emission signal exceeds a preset threshold during the observation interval was recorded; this parameter carries information about the cumulative damage to the test object as a result of external action [8, 12].

During the second loading cycle, the internal structure of synthetic quartz was studied using a GEOSKAN-2MU automated laser-ultrasonic structuroscope [13, 14] to make measurements from one side in an echo mode, detecting pores, micro-cracks and foreign inclusions. Fig. 1 shows its schematic diagram. Radiation (wavelength 1,06 μm, pulse duration 15 ns, maximum pulse energy $2 \cdot 10^{-4}$ J) from a solid-state laser (1), which operates in a Q-switched mode, is delivered, via a fiber optic cable (2), to an optical system (3) fixed on the housing of a photoacoustic transducer (4). The optical system forms a 2,5 mm-radius light beam that goes to a transparent plexiglas prism (5) with plane-parallel bases; the prism is subsequently used as an acoustic line for acoustic signals. Having passed through the prism, the laser light is absorbed by a plate 300 μm thick (6); the plate is attached to the prism and serves as an optoacoustic generator. The duration of the excited pulses is less than 100 ns, which corresponds to a spatial extent of less than 0,5 μm, judging from the speed of propagation of acoustic signals in rocks. The diameter of the ultrasonic beam is 2 mm, which is the same as that of the laser beam. Two pulses are excited by the opto-acoustic generator. The first pulse (a reference one) propagates in the prism and the second one (probing pulse) travels through the sample. All signals, i.e. the reference signal and signals reflected from a defect (8) and the opposite side of the sample, are recorded by a damped broadband piezoelectric transducer (9) and converted into electric signals, which are fed to an amplifier (10) and then processed by a computer (11).

Registered phase change of the acoustic signal indicates that there is a defect. Distance $h_d$ of the defect to the front side of the sample can be determined from delay $\Delta t_d$ f the signal reflected from the defect relative to the reference signal:

*Table 1*
***Physical and mechanical properties of test material***

| Axis | Longitu-dinal waves velocity $c_l$ (m/s) | Transverse wave velocity $c_t$ (m/s) | Elastic modulus $E_y$ (GPa) | Poisson ratio ν | Uniaxial compression strength $\sigma_c$ (MPa) |
|---|---|---|---|---|---|
| X | 5750 | 3360 | 74 | 0,24 | 300 |
| Y | 6010 | 4570 | 90 | 0,20 | 315 |
| Z | 6320 | 4680 | 104 | 0,11 | 350 |

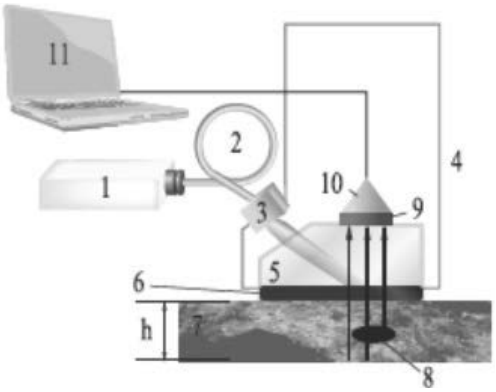


*Fig. 1. Schematic diagram of GEOSKAN-2MU structuroscope: 1 —* laser; *2 —* fiber optic cable; *3 —* optical system; *4 —* housing of optoacoustic transducer; *5 —* transparent prism; *6 —* black plastic plate; *7 —* geomaterial sample; *8 —* defect in sample; *9 —* damped piezoelectric receiver; *10 —* amplifier; *11 —* computer

$h_d = c_l \Delta t_d / 2$. Velocity $c_l$ of longitudinal acoustic wave in the formula is easily determined from delay $\Delta t_h$ of the signal reflected from the opposite side of the sample relative to the reference signal: $c_l = 2h / \Delta t_d$, where $h$ is the thickness of the test sample. The error in $h$ and $h_d$ was less than 0,5 % in our experiments. The short duration of the probing signal excited by the plate (6) allowed defects to be detected at a depth of over 0,2 mm. The «dead» zone was minimal. Scanning over the sample's surface with a step of less than 2 mm made it possible to obtain a 2D image of the internal structure of the sample.

The experimental curves were compared with the results of numerical simulation of the behavior of synthetic quartz under uniaxial compression. The numerical simulation was performed using Abaqus 6.13 Software whose Abaqus/Explicit module [15] considers the sample to be firmly fixed between the lower fixed plate and the upper movable one of the compression testing press. The plates were regarded as discrete rigid elements having the same size. Increments in the load applied to the upper plate to move the plate along the *Y* axis were simulated by an increase in the initial displacement of the plate at each time point. The numerical simulation was based on the Drucker-Prager model [16–18] that describes the behavior of material under load. The model takes the strength

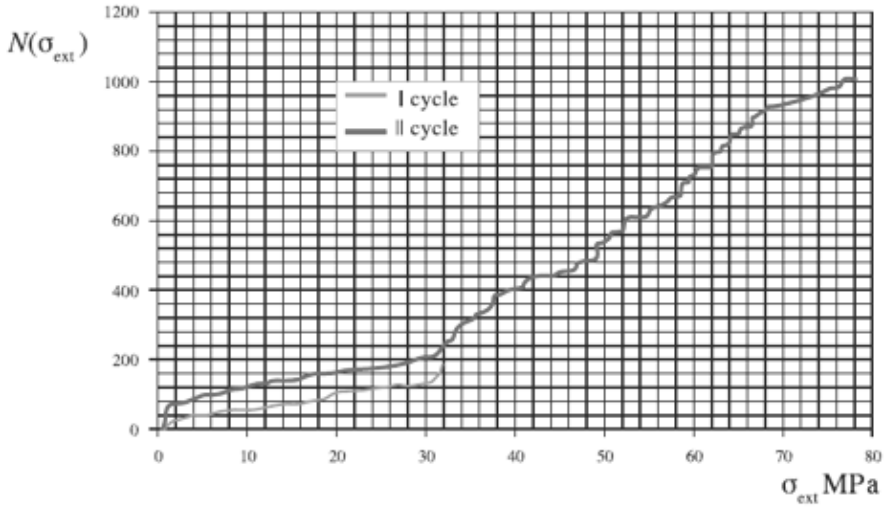


*Fig. 2. The number of times (N) the acoustic emission signal exceeds a preset threshold during the observation interval versus the applied stress ($\sigma_{ext}$) for two consecutive loading cycles*

characteristics into account, viz. specific weight $Y$ = 26,5 kN/m$^3$, elasticity modulus $E$ = 100 GPa, angle of internal friction $\varphi$ = 31°, angle of dilatancy $\psi$ = 20°, and compression strength $\sigma_c$ = 300 MPa.

**Results and discussion**

Fig. 2 shows typical $N$ vs. $\sigma_{ext}$ curves for two consecutive compressive loading cycles, where $N$ is the number of times the acoustic emission signal exceeds a preset threshold during the observation interval and $\sigma_{ext}$ is the external stress applied in the plane $Y$ = 0 along the $Y$ axis (see Fig. 3) parallel to the longest edge of the synthetic quartz sample.

During the first cycle, the behavior of the material under mechanical loading follows Hooke's law, and nonlinearity of $N(\sigma_{ext})$ at the end of the cycle is most probably due to the activation/evolution of existing two-dimensional, one-dimensional, and point defects in the material, not the formation of large defects. For the second loading cycle, there are two $\sigma_{ext}$ intervals, in which $N(\sigma_{ext})$ is virtually linear (except for the stage of preload) [19–21]. The values of $dN / d\sigma_{ext}$ significantly differ between these intervals. The increase in $dN / d\sigma_{ext}$ at $\sigma_{ext} \approx 30$ MPa is due to growth promotion of micro-defects that were initiated during the first loading cycle. They significantly increase in size during the second loading cycle. This is also confirmed by the fact that the sample exhibits an abrupt increase in acoustic emission, when kept under constant load at the end of the first cycle; the character of acoustic emission is largely determined by the presence of earlier formed defects.

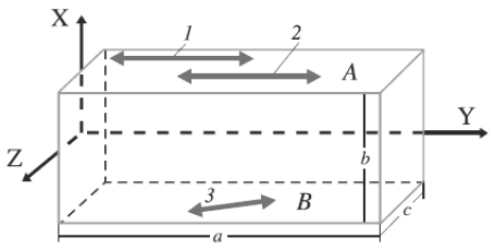


*Fig. 3. Geometry of sample and areas of laser-ultrasonic scanning. The origin of coordinates is at the center of the side edge of the parallelepiped*

After two consecutive cycles of compressive loading, synthetic quartz was investigated using a GEOSKAN-2MU structuroscope. The structuroscope can produce images of multiple microcracks formed mainly along the $Y$ axis in any cross-section perpendicular to one of the test sample's seven unloaded edges, when scanning along the line of intersection between an edge and the cross-section perpendicular to the edge (for example, along segments 1 and 2 when scanning along edge A, or along segment 3 when scanning along edge B of the sample shown in Fig. 3). The defect images obtained by scanning along segments 1 and 2 are shown in Fig. 4a and 4b, respectively. The darker narrow elongated areas with rough boundaries (corresponding to phase changes of the acoustic signal in reflection) are the images of microcracks formed after two consecutive loading cycles.

The study has shown that two consecutive cycles of loading cause structural defects 3mm in size throughout the synthetic quartz sample, not just near the plane $Y$ = 0 contacting with the press plate. In the near-surface region at a depth of 2 to 5 mm from the edges parallel to the planes $X$ = 0 and $Z$ = 0, numerous additional cracks up to 12 mm long occur near the surface subjected to loading (Fig. 4a). In the central region of the sample (Fig. 4b) cracks are still longer. They are mainly located near the $Y$ axis, and their length reaches 22 mm.

To verify the experimental results, numerical simulation of the behavior of a synthetic quartz crystal under uniaxial

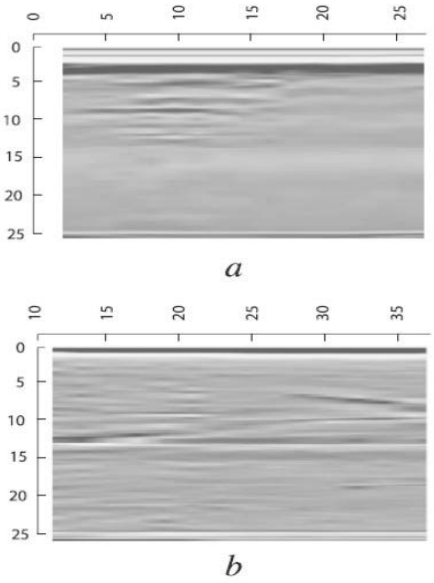


*Fig. 4. Scanning along segments 1 and 2 shown in Fig. 3:* a — the internal structure of the sample near its surface; b — in the middle of the sample

compression along the *Y* axis was performed. Fig. 5 shows the results of numerical simulation of the equivalent Mises stress

$$\sigma_M = \{[(\sigma_1 - \sigma_2)^2 + (\sigma_2 - \sigma_3)^2 + (\sigma_1 - \sigma_3)^2] / 2\}^{1/2}$$

[7, 16–18] obtained on the base of the Drucker-Prager model [9]. In last formulae $\sigma_1$, $\sigma_2$ and $\sigma_3$ are three principal normal stresses [7, 16–18] correspondingly ($\sigma_1 > \sigma_2 > \sigma_3$). The distribution of Mises stress is shown on the sample's faces parallel to the *Y* axis on the planes $X = b / 2$ and $Z = c / 2$ at an external load of 30 MPa. In the central part of the side edges and near the plane $Y = 0$, there are small areas with $\sigma_M$ three times greater than the normal stresses in other parts of the sample. Areas with the highest $\sigma_M$ are situated in the same sample pats in figures *a* and *b*.

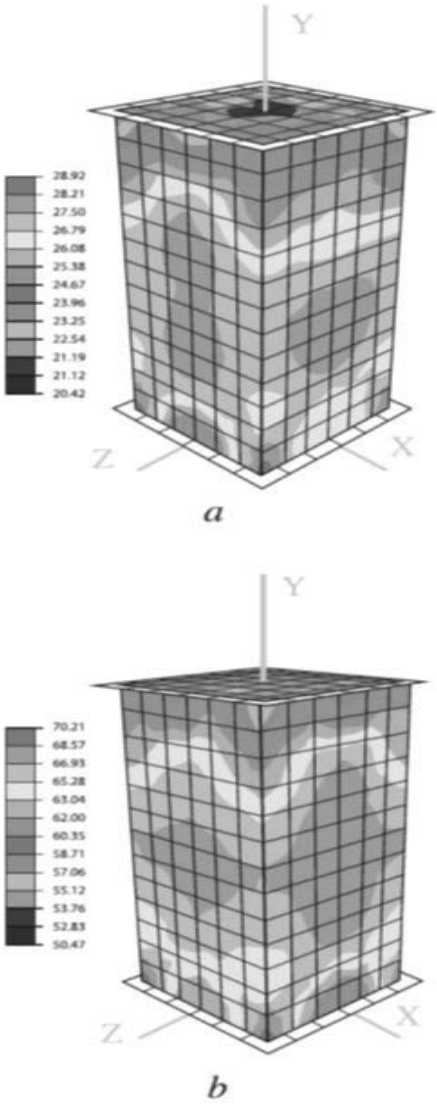


*Fig. 5. The simulated distribution of Mises stresses $\sigma_M$ across the sample's faces parallel to the Y axis (MPa) at an external load of 30 MPa (a) and 75 MPa (b)*

## Conclusions

The behavior of a synthetic quartz crystal whose properties are similar to those of natural rocks has been investigated under cyclic loading with the aid of acoustic emission and laser ultrasonic testing techniques using an automated GEOSKAN-2MU structuroscope. Two consecutive cycles of loading were performed, the longest edge of the crystal being oriented along the *Y* crystallophysical

axis. The experimental results were interpreted with the help of the numerical solution of the problem for a sample under uniaxial compression; the properties of the sample were described using the Drucker-Prager model, which takes the strength characteristics into account. The properties of the material, the heterogeneity of which is related to the presence of a small number of micro-defects and anisotropy, change at the early stages of mechanical loading. During repeated loading, earlier formed defects cause significant changes in the structure. After two consecutive loading cycles, defects up to 3 mm in size occur throughout the synthetic quartz crystal. In the near-surface region at a depth of 2 to 5 mm from the edges parallel to the planes $X = 0$ and $Z = 0$, numerous additional cracks up to 12 mm long occur (Fig. 4, a) near the surface subjected to the load. In the central area of the sample, cracks are mostly found near the $Y$ axis; their length reaches 22 mm. The further research could be conducted with a view to creating a model to take the non-linear dependence of strains and stresses on the external load into account.

## REFERENCES


1. *Preteseille M.*, *Lenoir T.* Mechanical fatigue behavior in treated/stabilized soils subjected to a uniaxial flexural test. *International Journal of Fatigue*, 2016, Vol. 14, pp. 1923—1929. DOI: 10.1016/j.trpro.2016.05.159.

2. González-*Cao J.*, *Varas F.*, *Bastante F. G.*, *Alejano L. R.* Ground reaction curves for circular excavations in non-homogeneous, axisymmetric strain-softening rock masses. *Journal of Rock Mechanics and Geotechnical Engineering*, 2013, Vol. 5, pp. 431—442. DOI: 10.1016/j.jrmge.2013.08.001.

3. *Jia L. C.*, *Chen M.*, *Zhang W.*, *Xu T.*, *Zhou Y.*, *Hou B.*, *Jin Y.* Experimental study and numerical modeling of brittle fracture of carbonate rock under uniaxial compression. *Mechanics Research Communications*, 2013, Vol. 50, pp. 58—62. DOI: 10.1016/j.mechrescom.2013.04.002.

4. *Xue L.*, *Qin S.*, *Sun Q.*, *Wang Y.*, *Lee L. M.*, *Li W.* A study on crack damage stress thresholds of different rock types based on uniaxial compression tests. *Rock Mechanics and Rock Engineering*, 2014, Vol. 47, pp. 1183–119. DOI: 10.1007/s00603-013-0479-3.

5. *Li X. Z.*, *Shao Z. S.*, *Fan L. F.* A micro-macro method for predicting the shear strength of brittle rock under compressive loading. *Mechanics Research Communications*, 2016, Vol. 75, pp. 13—19. DOI: 10.1016/j.mechrescom.2016.05.008.

6. *Brantut N.*, *Heap M. J.*, *Meredith P. G.*, *Baud P.* Time-dependent cracking and brittle creep in crustal rocks: A review. *Journal of Structural Geology*, 2013, Vol. 52, pp. 17—43. DOI: 10.1016/j.jsg.2013.03.007

7. Revil-*Baudard B.*, *Cazacu O.* Role of the plastic flow of the matrix on yielding and void evolution of porous solids: Comparison between the theoretical response of porous solids with Tresca and von Mises matrices. *Mechanics Research Communications*, 2014, Vol. 56, pp. 69—75. DOI: 10.1016/j.mechrescom.2013.11.008.

8. *Aker E.*, *Kühn D.*, *Vavryèuk V.*, *Soldal M.*, *Oye V.* Experimental investigation of acoustic emissions and their moment tensors in rock during failure. *International Journal of Rock Mechanics & Mining Sciences*, 2014, Vol. 70, pp. 286—295. DOI: 10.1016/j.ijrmms.2014.05.003.

9. *Lin J.*, *Shao J.*-F., *Kondo D.*. A two scale model of porous rocks with Drucker–Prager matrix: Application to a sandstone. *Mechanics Research Communications*, 2011, Vol. 38, pp. 602—606. DOI: 10.1016/j/mechrescom2011.08.005.

10. *Zhang X.*-P., *Wu S.*, *Afolagboye L. O.*, *Wang S.*, *Han G.* Using the point load test to analyze the strength anisotropy of quartz mica schist along an exploration adit. *Rock Mechanics and Rock Engineering*, 2015, Vol. 49, pp. 1967—1975. DOI: 10.1007/s00603-015-0792-0.

11. *Guzmana I. L.*, *Iskander M.*, *Bless S.* Observations of projectile penetration into a transparent soil. *Mechanics Research Communications*, 2015, Vol. 70, pp. 4—11. DOI: 10.1016/j.mechrescom.2015.08.008.

12. *Ohtsu M.* Acoustic emission (AE) and related non-destructive evaluation (NDE) techniques in the fracture mechanics of concrete. *Elsevier Inc.*, 2015, 318 p.

13. *Shibaev I. A.*, *Vinnikov V. A.*, *Stepanov G. D.* Determining elastic properties of sedimentary strata in terms of limestone samples by laser ultrasonics. *MIAB. Mining Inf. Anal. Bull.* 2020, No. 7, pp. 125—134. [In Russ]. DOI: 10.25018/0236-1493-2020-7-0-125-134.

14. Shibaev, I. A., Morozov, D. V., Dudchenko, O. L., Pavlov, I. A. Estimation of local elastic moduli of carbon-containing materials by laser ultrasound. *Key Engineering Materials*, 2018, Vol. 769, pp. 96—101. DOI: 10.4028/www.scientific.net/KEM.769.96.

15. Abaqus 6.13 (Abaqus/CAE User's Guide), available at http://130.149.89.49:2080/v6.13/index.html, 2020.

16. *Yang Q.*, *Zhang J.*-M., *Zheng H.*, *Yao Y.* Constitutive Modeling of Geomaterials. *Springer Series in Geomechanics and Geoengineering,* 2013, 810 p.

17. *Oka F.*, *Murakami A.*, *Uzuoka R.*, *Kimoto S.* Computer Methods and Recent Advances in Geomechanics. *CRC Press*, 2014, 472 p.

18. *Jiang J.*-F., Wu Yu-F. Identification of material parameters for Drucker–Prager plasticity model for FRP confined circular concrete columns. *International Journal of Solids and Structures*, 2012, Vol. 49, pp. 445–456. DOI: 10.1016/j.ijsolstr.2011.10.002.

19. Practical Acoustic Emission Testing, *Springer*, 2016, 110 p.

20. *Zhou J. W.*, *Xu W. Y.*, *Yang X. G.* A microcrack damage model for brittle rocks under uniaxial compression. *Mechanics Research Communications*, 2010, Vol. 37, pp. 399—405. DOI: 10.1016/j.mechrescom.2010.05.001.

21. *Stoeckhert F.*, *Molenda M.*, *Brenne S.*, *Alber M.* Fracture propagation in sandstone and slate — Laboratory experiments, acoustic emissions and fracture mechanics. *Journal of Rock Mechanics and Geotechnical Engineering*, 2015, Vol. 3, pp. 237—249. DOI: 10.1016/j.jrmge.2015.03.011. ГИАБ

## ИНФОРМАЦИЯ ОБ АВТОРАХ

*Ян Прушка*[1] — доцент;
*Александр Кравцов*[1] — PhD, kravtale@fsv.cvut.cz;
*Сас Иван Евгеньевич*[2] — инженер;
*Черепецкая Елена Борисовна*[2] — доктор технических наук, профессор;
*Виего Жозе Викторина*[2] — студент;
*Борисов Никита Геннадьевич*[2] — аспирант;
[1] Чешский технический университет в Праге, строительный факультет, Thákurova 7/2077, Прага 6 — Дейвице, Чешская Республика;
[2] Национальный Исследовательский Технологический Университет «МИСиС» Горный институт, Москва, Россия.

## INFORMATION ABOUT THE AUTHORS

*Jan Pruška*[1], Assistant professor;
*Kravcov A. N.*[1], PhD, kravtale@fsv.cvut.cz;
*Sas I. E.*[2], engineer;
*Cherepetskaya E. B.*[2], Dr. Sci. (Eng.), Professor;
*Viegas Jose Victorino*[2], student;
*Borisov N. G.*[2], PhD-student;
[1] Czech Technical University in Prague, Faculty of Civil Engineering, Thákurova 7/2077, Prague 6 — Dejvice, 166 29, Czech Republic;
[2] National Research Technological University «MISiS» , Moscow, Russia.

Получена редакцией 20.01.2021; получена после рецензии 25.02.2021; принята к печати 10.03.2021.
Received by the editors 20.01.2021; received after the review 25.02.2021; accepted for printing 10.03.2021.